Repulsive axon guidance molecule Slit3 is a novel angiogenic factor

Bing Zhang,[1] Ursula M. Dietrich,[2] Jian-Guo Geng,[3] Roy Bicknell,[4] Jeffrey D. Esko,[5] and Lianchun Wang[1]

[1]Complex Carbohydrate Research Center, Department of Biochemistry and Molecular Biology, University of Georgia, Athens; [2]Department of Small Animal Medicine & Surgery, College of Veterinary Medicine, University of Georgia, Athens; [3]Vascular Biology Center, Division of Hematology, Oncology and Transplantation, Department of Medicine, University of Minnesota Medical School, Minneapolis; [4]Cancer Research UK Angiogenesis Group, Institute for Biomedical Research, University of Birmingham Medical School, Edgbaston, United Kingdom; and [5]Department of Cellular and Molecular Medicine, Glycobiology Research and Training Center, University of California San Diego, La Jolla

Slits are large, secreted repulsive axon guidance molecules. Recent genetic studies revealed that the Slit3 is dispensable for neural development but required for non-neuron–related developmental processes, such as the genesis of the diaphragm and kidney. Here we report that Slit3 potently promotes angiogenesis, a process essential for proper organogenesis during embryonic development. We observed that Slit3 is expressed and secreted by both endothelial cells and vascular smooth muscle cells in vasculature and that the Slit cognate receptors Robo1 and Robo4 are universally expressed by endothelial cells, suggesting that Slit3 may act in paracrine and autocrine manners to regulate endothelial cells. Cellular function studies revealed that Slit3 stimulates endothelial-cell proliferation, promotes endothelial-cell motility and chemotaxis via interaction with Robo4, and accelerates endothelial-cell vascular network formation in vitro with a specific activity comparable with vascular endothelial growth factor. Furthermore, Slit3 stimulates neovessel sprouting ex vivo and new blood vessel growth in vivo. Consistent with these observations, the Slit3 knockout mice display disrupted angiogenesis during embryogenesis. Taken together, our studies reveal that the repulsive axon guidance molecule Slit3 is a novel and potent angiogenic factor and functions to promote angiogenesis in coordinating organogenesis during embryonic development. (Blood. 2009;114: 4300-4309)

Introduction

The axon guidance molecule Slits are large, secreted proteins and are highly conserved from *Caenorhabditis elegans* to vertebrates.[1-4] Mammals have 3 Slit proteins (Slit1-3). Slits bind to Robo receptors to induce repulsive signaling during axon guidance and neuronal migration.[5,6] Slit1-3 show both overlapping and distinct expression patterns.[7-9] Slit1 and Slit2 are expressed prominently in the central nervous system. In contrast, Slit3 is widely expressed in the central nervous system and peripheral tissues and organs, such as the developing tongue, kidney, genital ridge, pharynx, umbilical cord vein, atrial wall of heart, lung, and diaphragm.[7-9] Consistent with the expression patterns, the authors of mouse genetic studies[8-10] have established that Slit1 and Slit2 are essential for neural development, whereas Slit3 is dispensable. Instead, Slit3 is required for diaphragm and kidney genesis, revealing that Slit3 critically regulates non-neuron–related developmental processes.[8,9]

Angiogenesis refers to the generation of new blood vessels from existing capillary plexus in response to angiogenic stimuli.[11-13] Angiogenesis is finely orchestrated, in which growing vessels navigate through a complex extracellular environment to their target sites in a tightly controlled series of guidance decisions.[14] During embryonic development, growing blood vessels and navigating nerves are in close proximity, resemble each other, and follow similar routes to form branching networks, suggesting that vascularization and innervation may share common mechanisms in choosing and following specific paths to reach their respective destinations.[14,15] The patterning of nerves is regulated by attractive and repulsive guidance cues.[14,16] Four major families of neuronal guidance factors have been identified, including semaphorin, ephrin, netrin, and slit, along with their cognate receptors, nurophilin, Eph, uncoordinated-5, and Robo.[16] The authors of recent genetic studies[17-19] observed that ephrin-B2, semaphorin, and netrin critically control angiogenesis in vitro and in vivo, demonstrating that common molecular mechanisms are truly shared by vascularization and innervation.

The Slit–Robo interaction is implicated in angiogenesis as well.[15,20-22] Slit2 was found to interact with Robo1 and Robo4, which are expressed by endothelial cells (ECs) to modulate EC migration and to participate in tumor angiogenesis, thus demonstrating that Slit2 directly modulates angiogenesis. *Slit3* was reported to be expressed in vessels[23,24]; however, the role of Slit3 in angiogenesis is not known. In this study, we examined the angiogenic effect of Slit3 and demonstrated that Slit3 is a novel and potent angiogenic factor. Our studies also demonstrate that Slit3 promotes developmental angiogenesis to accommodate organogenesis during mammalian development.

Methods

Immunohistochemical analysis, cell culture, and transcript analysis

The immunostaining of mouse tissue sections and the isolation and culture of ECs and vascular smooth muscle cells (VSMCs)[25-28] are described in the

Submitted December 11, 2008; accepted August 18, 2009. Prepublished online as *Blood* First Edition paper, September 9, 2009; DOI 10.1182/blood-2008-12-193326.

The online version of this article contains a data supplement.

The publication costs of this article were defrayed in part by page charge payment. Therefore, and solely to indicate this fact, this article is hereby marked "advertisement" in accordance with 18 USC section 1734.

supplemental Methods (available on the *Blood* website; see the Supplemental Materials link at the top of the online article). The University of Georgia Institutional Animal Care and Use Committee approved our use of both mice and rats for these studies.

RT-PCR analysis

Total RNA of cells was extracted with RNeasy Kit (Qiagen) and reverse-transcribed by Improm-II Reverse Transcription System (Promega). The RT-PCR primers were designed by the use of Primer Designer 1.0 software with Tm at approximately 60°C. Primer pairs for *Slit1-3*, *Robo1-4*, and *vascular endothelial growth factor* (*VEGF*) are listed in the supplemental Methods. Real-time reverse-transcription polymerase chain reaction (RT-PCR) was performed by the use of the IQ SYBR Green real-time PCR Kit (Bio-Rad) following the manufacturer's instructions. Cycle threshold values from triplicate assays were collected to calculate fold expression compared with *Slit3* expression in the same sample.

Transfection, immunoprecipitation, Western blot, and F-actin staining

Plasmids encoding full-length human *Slit3-myc*, *Robo1-HA*, *Robo4-HA*, or control empty vectors were transfected into HEK 293 cells. Conditioned medium (CM) from the *Slit3-myc* or control vector–transfected cells were collected 72 hours after the transfection and concentrated by the use of a Biomax-100K ultra-free filter (Millipore). Lysate from the cells transfected with *Robo1-HA*, *Robo4-HA*, or control vector were prepared with lysis buffer (0.5% NP-40; 50 mmol/L Tris, pH 7.5; 150 mmol/L NaCl; 1 mmol/L ethylene diamine tetraacetic acid; 50 mmol/L sodium fluoride; 1 mmol/L Na_3VO_4; 1 mmol/L dithiothreitol; 1 mmol/L phenylmethylsulphonyl fluoride; 25 μg/mL aprotinin; 25 μg/mL leupeptin, and 150 μg/mL benzamidine), and mixed with the collected CM. The Slit3–Robo complex was pulled down by agarose beads conjugated with anti-HA antibody (Santa Cruz Biotechnology Inc) and analyzed by Western blot with the use of anti-Myc antibody (Santa Cruz Biotechnology Inc).[22,29] For F-actin staining, subconfluent human umbilical vein ECs (HUVECs) grown on slide chambers were fixed with 4% paraformaldehyde and permeabilized in 0.1% Triton-X100 in phosphate-buffered saline. After washing, the cells were stained with tetramethylrhodamine isothiocyanate (TRITC)–phalloidin (Molecular Probes) in 0.1% Triton-X100. Cell cytoskeleton images were acquired by an Olympus confocal microscope (Olympus).

Cell proliferation

The mitogenic activity of Slit3 on ECs was measured by the CellTiter 96 AQ One solution cell proliferation assay (Promega). In brief, ECs at 10^3 per well were seeded to a 96-well plate. After serum starvation for 16 hours, the cells were cultured in media containing 0.5% fetal bovine serum and test factors (bovine serum albumin [BSA], Slit3, VEGF, or fibroblast growth factor [FGF]-2) for 2 days. After the addition of the CellTiter 96 AQ One solution and incubation for an additional 1 hour, the absorbance at 490 nm was measured by the use of an OPTI-microplate reader (Thermo Electron Corp). The cell proliferation rate was determined by the fold increase of the absorbance over BSA control.

Cell motility

Cell motility was assessed by the wound healing assay and Boyden Chamber Transwell analysis as described in the supplemental Methods.[27] For Robo functional blocking experiments, test antibodies (1 μg/well),[21,30] soluble extracellular domain of Robo1, soluble extracellular domain of Robo4,[20] or proper controls were added to the lower chamber.

Rho GTPase activity analysis

Rac1, RhoA, and Cdc42 activities were assessed following the protocols of the EZ-Detect Rho GTPase assay Kit (Pierce) and are described in the supplemental Methods.

EC tube formation

HUVECs (3×10^4 cells/well) suspended in EBM-2 medium containing BSA (1.3 nmol/L), Slit3 (0.8 nmol/L), VEGF (1.5 nmol/L), or FGF-2 (1.8 nmol/L) were seeded on growth factor-reduced matrigel coated 48-well culture plates.[25,27] After 6 hours in culture, capillary-like tube formation was photographed by a phase contrast microscope. Total tube length (TTL) of the formed tubes was quantified by ImageJ software.

Rat aortic ring assay

Thoracic aortas harvested from 2-month-old Fisher-344 male rats (Harlan) were cut into 1- to 2-mm small pieces, placed into 48-well plates precoated with matrigel, and then covered with another layer of matrigel.[31] After gelatinization, serum-free EBM-2 media containing BSA (1.3 nmol/L), Slit3 (0.8 nmol/L), VEGF (1.5 nmol/L), or FGF-2 (1.8 nmol/L) was applied. The microvessel sprouting from the adventitial layer of the aortic ring was photographed on day 7. The sprouting vessels were ranked using the following scale: 0, no sprouting; 0.25, isolated sprouting; 0.5, sprouting in 20% to 50% of the arterial circumference; 1, sprouting in 50% to 75% of the circumference; 1.5, sprouting in 100% of the circumference; and 2, 100% of the artery circumference occupied by sprouts longer than one-third of the length of the average radius of the rings.

Chorioallantoic membrane (CAM) assay

In brief, fertilized specific pathogen-free eggs (Charles River) were incubated in an egg incubator at 37°C, with 60% humidity and constant fresh air.[32] On day 3, a window (1 cm × 1 cm) right above the embryo was opened and sealed with dual-pore film (Denville Scientific). On day 8, 1-mm^3 Gelfoam sponge (Upjohn) soaked with test growth factors was applied onto the CAM through the established window and incubated for another 3 days. The CAM around the graft was then fixed with 4% fresh paraformaldehyde, cut out, and photographed under a dissection microscope (SMZ 1500, Nikon). The microvessels that moved toward the grafts were counted by blinded reviewers.

Corneal micropocket angiogenesis assay

Corneal micropocket angiogenesis assay was performed as previously described.[33] In brief, slow-releasing pellets were prepared by homogeneously mixing test factors with sucralfate and 12% hydron (both from Sigma-Aldrich). To implant the pellets into mouse cornea, 6- to 8-week-old C57BL/6 mice (the Jackson laboratory) were anesthetized with Avertin (400 mg/kg, Sigma-Aldrich). The animals were placed in lateral recumbency, and the globe was carefully proptosed by retracting the lids with straight tying forceps. By using an operating microscope (Wild/Leica M691, Endure Medical) and a von Graefe knife No. 3, we placed a 0.3- to 0.4-mm linear, midstromal incision in the center of the cornea. A micropocket was then created from the incision toward the lateral limbus with sliding motions of the microknife and with care not to perforate the cornea. A pellet was implanted into the micropocket, and topical erythromycin ointment was applied. After 5 days, the corneas were examined with slit-lamp biomicroscopy (SL14) and photographed under a dissection microscope (Nikon). The neovascularization in mouse corneas was quantified using the formula: 0.063 × vessel length (mm) × clock hour using ImageJ software.

Results

Slit3, *Robo1*, and *Robo4* are coexpressed in vasculature

Slit was observed to express in ECs; however its expression profiles are unclear.[9,21,23] This was examined at first by semiquantitative RT-PCR analysis. As shown in Figure 1A, *Slit2* and *Slit3* were highly expressed in HUVECs and in the primary ECs isolated from mouse lung and diaphragm but not liver. The expression pattern and abundance of *Slit1-3* in HUVECs and in the primary mouse

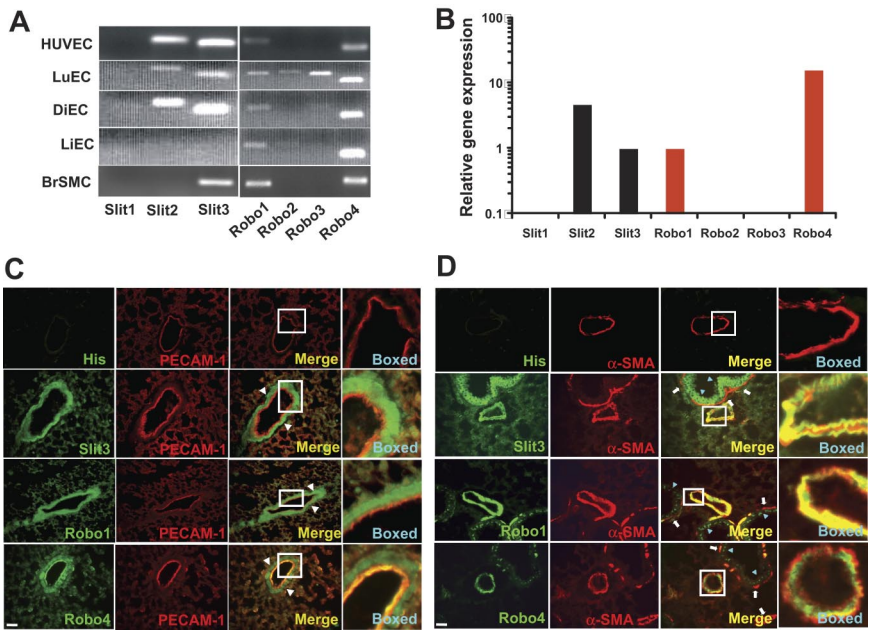

Figure 1. *Slit3*, *Robo1*, and *Robo4* are expressed in vasculature. (A) Semiquantitative RT-PCR analysis determined the mRNA transcripts of *Slit1-3* and *Robo1-4* in HUVECs, primary mouse ECs from lung (LuEC), diaphragm (DiEC), and liver (LiEC), and primary rat brain VSMCs (BrSMC). (B). Real-time RT-PCR analyses of the expression profile of *Slit1-3* (black bars) and *Robo1-4* (red bars) in HUVECs. The data are presented relative to the *Slit3* expression. (C-D). Coimmunostaining. Cryosections of adult mouse lung tissues were immunostained with anti-PECAM-1 (red), anti-α-SMA (red), and anti-His, anti-Slit3, anti-Robo1, or anti-Robo4 (all green) antibodies. Slit3, Robo1, and Robo4 colocalized with PECAM-1 (merged), whereas no anti-His staining was observed, showing that the staining of Slit3, Robo1, and Robo4 were specific. Cells outside PECAM-1–positive cells were observed to also express Slit3, Robo1, and Robo4 (indicated by white arrowhead), suggesting that Slit3 may also be expressed by VSMCs. This was confirmed by the colocalization of α-SMA with Slit3, Robo1, and Robo4 (merged) in vasculature. The colocalization of Slit3, Robo1, and Robo4 with PECAM-1 or α-SMA in the boxed areas in the merged images are shown at a higher magnification. High level of Slit3 and low levels of Robo1 and Robo4 are expressed by epithelial cells of bronchium (indicated by light blue arrowhead) but not bronchial SMCs (arrow), which express only low levels of Robo1 and Robo4. Scale bar, 120 μm.

lung, liver, and diaphragm ECs were further confirmed by real-time RT-PCR analysis (Figure 1B and data not shown). To visualize Slit3 protein in vasculature, cryosections of mouse tissues were double stained with anti-mouse platelet-EC adhesion molecule-1 (PECAM-1), a marker specific for ECs, and specific anti-Slit3 (supplemental Figure 1) antibodies. Consistent with the mRNA transcript analysis, Slit3 was highly expressed in ECs in the lung and brain of adult mice (Figure 1C; supplemental Figure 2A-D). However, the endothelial Slit3 expression was low in kidney and not in the liver (supplemental Figure 2I-N) and heart (data not shown). Furthermore, colocalization staining observed that Slit3 also was abundantly expressed in the cells outside of the EC layer, indicating that VSMCs also express Slit3 (Figure 1C; supplemental Figure 2A-D). This was confirmed by semiquantitative and real-time RT-PCR analyses of rat brain VSMCs (Figure 1A; data not shown), and by coimmunostaining mouse lung and brain tissue with anti-α-smooth muscle actin (anti-α-SMA), a specific marker for SMCs (Figure 1D; supplemental Figure 2E-H). To further determine whether the expressed Slit3 can be secreted, an enzyme-linked immunosorbent assay (ELISA) method was developed in which recombinant Robo1 protein was coated onto plates and bound Slit3 was detected with specific anti-Slit3 antibody. By the use of this method, Slit3 was detected in the CM collected from mouse lung ECs, HUVECs, and VSMCs (supplemental Figure 2O), suggesting that Slit3 can be secreted into the extracellular matrix from both ECs and VSMCs in vasculature.

Robos are the putative receptors for Slits, and their expression profile in vasculature also has not been clearly defined.[20-22,34,35] By using semiquantitative and real-time RT-PCR analyses, we observed that HUVECs and the primary ECs isolated from mouse lung, diaphragm, and liver universally express low levels of *Robo1* and high levels of *Robo4* (Figure 1A). In addition, mouse lung ECs also expressed *Robo2* and *Robo3* (Figure 1A). In situ immunostaining and Western blot analysis of EC lysates further confirmed endothelial expression of Robo1 and Robo4 (Figure 1D; supplemental Figure 2P). Given that Slit3 is secreted in vasculature, this observation suggests that Slit3 may interact with endothelial Robos to modulate EC function in angiogenesis.

Slit3 is an EC mitogen

To determine whether Slit3 modulates EC functions, we first tested whether Slit3 is an EC mitogen. Because full-length Slit3 protein is not available, we used a purified, recombinant mouse Slit3 fragment, which contains the biologically active leucine-rich repeat regions (Ser27-His901, R&D Systems). Slit3 was supplemented in primary EC culture at 0 to 0.4 nmol/L. After 2 days, the cell numbers were determined. As shown in Figure 2, compared with

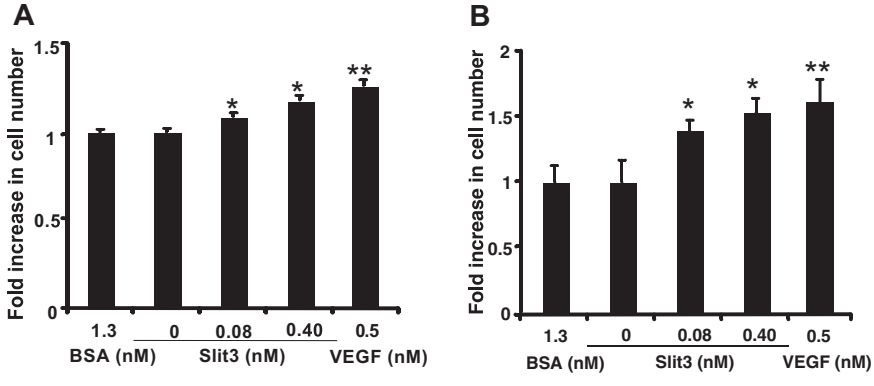

Figure 2. Slit3 stimulates EC proliferation. The cell number of the cultured mouse lung ECs (A) and HUVECs (B) was measured after the addition of recombinant Slit3 at 0 to 0.40 nmol/L in the culture medium. BSA (1.3 nmol/L) served as a negative control, whereas VEGF (0.50 nmol/L) served as a positive control. The data are presented as -fold increase in cell number relative to the BSA control. The results were from 3 independent experiments in triplicate and are expressed as mean ± SD. Asterisks indicate the treatment that yielded statistically significant differences in comparison with BSA control (*$P < .05$; **$P < .005$, Student *t* test).

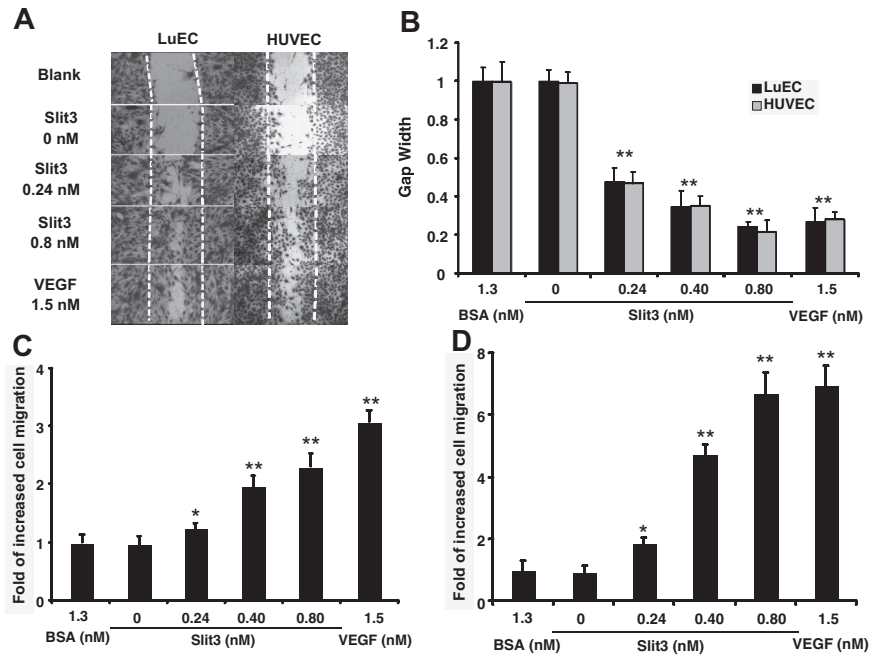

Figure 3. Slit3 promotes EC motility and migration. (A-B) Wound healing assay. The confluent EC monolayer was scratched to create a wounded gap (highlighted by the dashed lines) and then cultured with a supplement of BSA (1.3 nmol/L), recombinant Slit3 (0-0.80 nmol/L), or VEGF (1.5 nmol/L). After 24 hours, the gap width relative to the ones cultured with BSA was quantified. (C-D) Modified Boyden Chamber assay. BSA, Slit3, or VEGF was supplemented in the lower chamber, with HUVECs (C) or mouse lung ECs (D) loaded in the upper chamber. The data are presented as the -fold increase in number of cells migrated to the bottom side of the chamber relative to the BSA control. Data are summarized from at least 3 independent experiments in triplicate and presented as mean ± SD. Asterisk indicates statistical difference compared with the BSA treatment by Student *t* test (*$P < .01$; **$P < .001$).

BSA treatment (1.3 nmol/L, negative control), both mouse ECs and HUVECs showed dose-dependent mitogenic responses to Slit3. The mitogenic activity of 0.4 nmol/L Slit3 was comparable with 0.5 nmol/L VEGF, a well-known EC mitogen. Cell cycling analysis found that Slit3 stimulated more ECs in the M phase and did not induce EC apoptosis (data not shown), indicating that the proliferating effect of Slit3 was caused by accelerating EC mitosis. In conclusion, these observations demonstrate that Slit3 is a potent EC mitogen.

Slit3 is chemoattractant for ECs

During angiogenesis, high EC motility is critically required for vessel sprouting to form new vasculature.[11,14,36] Slit2 was observed to modulate cell motility, and this function is conserved among various cell types, including neuronal cells, ECs, and leukocytes.[10,21-23] Recently, Slit3 was implicated in modulating the motility of macrophages.[37] These observations suggest that Slit3 may also modulate EC motility. Cell motility includes 2 types of cell movement, the autonomous migration and chemotaxis. We initially examined whether Slit3 is able to enhance EC autonomous migration by supplementing Slit3 in culture in the cell-wounding assay. VEGF, a growth factor known to promote EC motility, and BSA were used as positive and negative controls, respectively. The migration of ECs from the wounded edge into the denudated area was quantified by measurement of the gap width. As shown in Figure 3A, compared with the BSA treatment (1.3 nmol/L), Slit3 dose dependently promoted EC migration into the wounded area. Quantification revealed that after 24 hours of the treatment, the gap width of 0.8 nmol/L Slit3-treated wells was comparable with that of 1.5 nmol/L VEGF (0.36 ± 0.06 for Slit3 vs 0.28 ± 0.04 for VEGF, $P > .50$), thus showing that Slit3 vigorously promotes EC motility (Figure 3B). To determine whether Slit3 induces EC chemotaxis, the Boyden Chamber assay was carried out by supplementing Slit3, VEGF, or BSA in the lower chamber with ECs loaded in the upper chamber. The ECs that migrated onto the bottom side of the Transwell were counted. As shown in Figure 3C-D, Slit3 dose dependently promoted EC transmigration. At 0.8 nmol/L, Slit3 induced a 6.5-fold increased migration of mouse lung ECs and a 2.5-fold increased migration of HUVECs, showing a chemotactic activity comparable with VEGF at 1.5 nmol/L (6.9- and 3.0-fold increased migration of mouse lung ECs and HUVECs, respectively; Figure 3C-D). Together, these observations revealed that Slit3 potentially enhances both autonomous migration and chemotaxis of ECs, exhibiting that Slit3 is a potent chemoattractant for EC migration.

Slit3 does not alter VEGF expression in ECs

Among the many factors implicated in angiogenesis, VEGF has been identified as the most potent and predominant angiogenic factor. Many molecules induce angiogenesis through stimulation of VEGF biosynthesis and function as indirect proangiogenic factors, such as fibroblast growth factor-4.[38] To test whether Slit3 stimulates *VEGF* secretion and/or augments VEGFR2 expression to induce EC proliferation and migration, the expressions of *VEGF* and *VEGFR2* in HUVECs were examined before and after treating with Slit3 for 12 and 24 hours in culture. As shown in Figure 4A to C, the Slit3 treatment did not alter *VEGF and VEGFR2* expression at transcript and protein levels, suggesting that Slit3 directly regulates EC functions.

Slit3 interacts with Robo4 to mediate endothelial chemoattractance

Slits interact with their cognate Robo receptors to mediate the biologic functions.[5,14] ECs universally express *Robo1* and *Robo4*, suggesting that Slit3 may interact with Robo1 and/or Robo4 to regulate EC functions. To test this hypothesis, we initially examined whether Slit3 interacts with Robo1 and Robo4. We observed that Slit3 coimmunoprecipitated with both Robo1 and Robo4 (Figure 4D). This observation was further supported by positive EC surface binding of Slit3 (Figure 4E-F). To determine whether Slit3 interacts with Robo1 and Robo4 directly, we further examined the binding of Slit3 to Robo1 and Robo4 by ELISA by using purified recombinant Slit3, Robo1, and Robo4 proteins. We observed that Slit3 dose dependently bound to immobilized Robo1 and Robo4

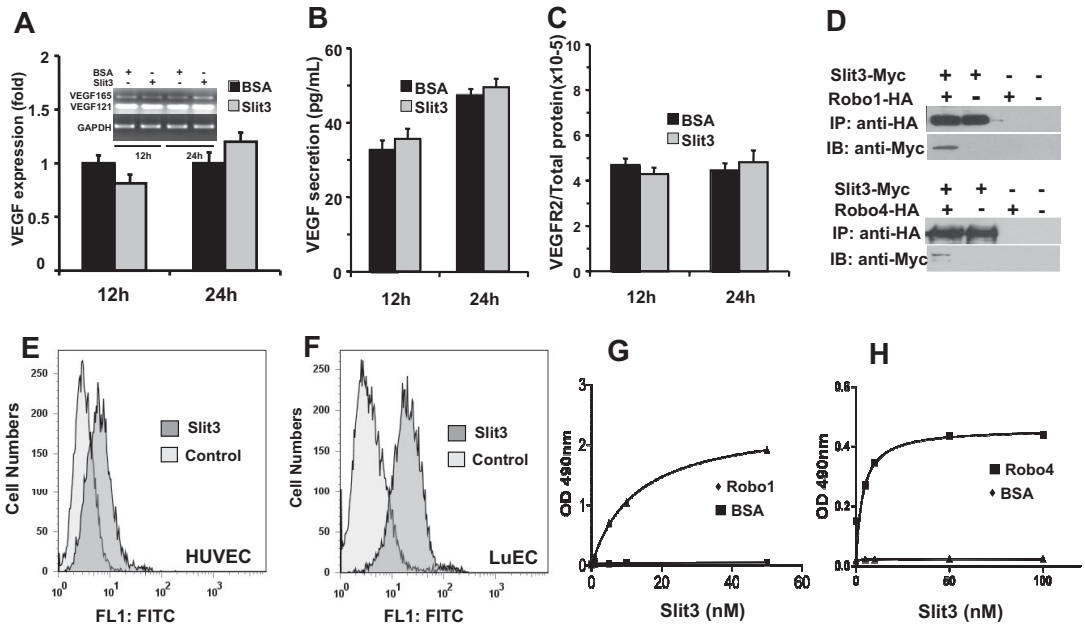

Figure 4. Slit3 has no effect on VEGF/VEGFR2 expression, binds on the EC surface, and interacts with both Robo1 and Robo4. (A-C) Slit3 treatment does not alter *VEGF/VEGFR2* expression in HUVECs. The expression of *VEGF121* and *VEGF165* transcripts in HUVECs were determined by quantitative RT-PCR analysis after adding Slit3 or negative control BSA (both at 0.8 nmol/L) in culture for 12 and 24 hours. Glyceraldehyde 3-phosphate dehydrogenase was used as a loading control. The expression of VEGF and VEGFR2 proteins was measured by ELISA. The comparison between BSA and Slit3 treatment at each test time point was analyzed by the Student *t* test with $P > .05$ having no statistical significance. (D) Slit3 coimmunoprecipitated with Robo1 and Robo4. CM from *Slit3-Myc* or the empty control vector transfected cells were mixed with *Robo1-HA*, *Robo4-HA*, or empty control vector–transfected cell lysate. The Slit3–Robo complex was immunoprecipitated (IP) by anti-HA antibody conjugated agarose beads and then immunoblotted (IB) with anti-Myc antibody. (E-F) Slit3 binds on the EC cell surface. The HUVECs and mouse lung ECs (LuEC) were incubated with Slit3. After further incubation with anti-Slit3 antibody and the fluorescein isothiocyanate–conjugated secondary antibody sequentially, the cell surface–bound Slit3 was measured by flow cytometer. The cells that were only incubated with the anti-Slit3 antibody and the fluorescein isothiocyanate–conjugated secondary antibody served as background control. Slit3 showed strong binding on cell surfaces of both HUVECs and LuECs. (G-H) Slit3 interacts directly with Robo1 and Robo4. In ELISA assays, Slit3 was incubated in Robo1- (G), Robo4- (H), or BSA-coated wells and bound to the immobilized Robo1 and Robo4 but not BSA. The data presented are representative of the experiments carried out at least 3 times in triplicate.

(Figure 4G-H) and that soluble Robo1 and Robo4 dose dependently bound to immobilized Slit3 (supplemental Figure 3A-B). Taken together, these examinations showed that Slit3 interacts with both Robo1 and Robo4, confirming and also extending previous findings.[20,39,40]

To test whether the Slit3–Robo interaction modulates EC function, we applied the Slit3-induced EC chemotaxis assay as the readout. The functional blocking anti-Robo1, anti-Robo4 (supplemental Figure 3C-D), or nonimmune antibody from the same animal species was supplemented into the Slit3- or VEGF-containing bottom chambers of the assay. As shown in Figure 5A, the nonimmune and the anti-Robo1 antibodies had no effect on Slit3-induced EC migration. In sharp contrast, the anti-Robo4 antibody completely inhibited the Slit3-induced EC migration. Furthermore, all the antibodies did not affect VEGF-induced EC migration, indicating that the blocking effect of the anti-Robo4 antibody was specific. We also carried out the experiment with R5, a monoclonal antibody that binds to the first immunoglobulin domain of Robo1 and blocks Slit2-Robo1 interaction,[21,30] and observed that the R5 did not inhibit the Slit3-induced EC migration either (data not shown), confirming that the Slit3-induced EC migration does not depend on Robo1. To alternatively confirm these observations, we also repeated the experiments by using the soluble extracellular domain of Robo1 or Robo4, which blocks Robo1- and Robo4-mediated biologic functions, respectively.[20,21] As shown in Figure 5B, soluble Robo4 strongly inhibited Slit3-induced EC migration, whereas soluble Robo1 had no effect. Furthermore, soluble Robo4 did not affect VEGF-elicited EC migration, further confirming that the inhibitory effect was Robo4 specific (Figure 5B). In summary, these experiments supported each other and revealed that Slit3 interacts with Robo4, but not Robo1, to induce EC motility.

Slit3 was observed to be secreted from both ECs and VSMCs (supplemental Figure 2O). Therefore, we also tested whether the endogenous Slit3 interacts with Robo4 to induce EC chemotaxis. We observed that the serum-free CMs collected from HUVEC and VSMC cultures both induced EC migration, and the promigratory function was partially inhibited by functional blocking anti-Robo4 antibody (Figure 5C), suggesting that the Slit3–Robo4 interaction occurs to modulate EC function in vivo.

Slit3 triggers Rho GTPase activation and cytoskeleton dynamics

Robo4 activation elicits Rho GTPase signaling, which results in alternations of cytoskeleton organization, polarity, and motility of ECs after the binding of unknown ligands.[41] Therefore, we further tested whether Slit3-Robo4 interaction triggers a similar intracellular signaling to promote EC motility. We measured endogenous GTP-bound RhoA, Cdc42, and Rac1 of the Rho GTPase family in ECs upon Slit3 stimulation by the GST-pull down assays. As shown in Figure 5D, Slit3 elicited a rapid increase of Rac1 and RhoA activation. The stimulated activation peaked at 5 minutes and 15 minutes for Rac1 and RhoA, respectively. Afterward, the RhoA signaling returned to basal levels within 60 minutes, whereas Rac1 signaling declined but remained activated through all the time period examined. No significant Cdc42 activation was observed. To determine whether Slit3 interacts with Robo4 to activate the Rho GTPases, HUVECs were stimulated with Slit3 in the presence of the functional blocking anti-Robo4 antibody. We observed that the

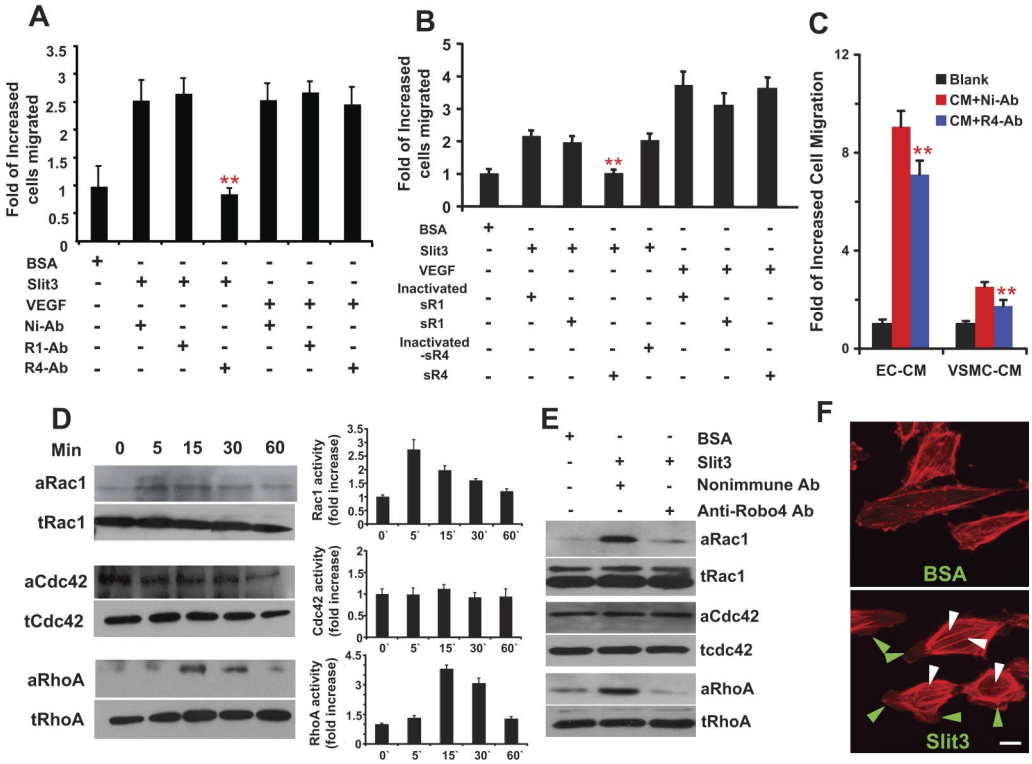

Figure 5. Slit3 interacts with Robo4 but not Robo1 to induce EC chemotaxis and Rho GTPases activation and triggers intracellular actin cytoskeleton reorganization. (A) Anti-Robo4 but not anti-Robo1 antibody blocked Slit3-induced EC migration. Nonimmune antibody (Ni-Ab, 1 μg), functional blocking anti-Robo1 (R1-Ab, 1 μg), or functional blocking anti-Robo4 (R4-Ab, 1 μg) antibody was supplemented in the bottom chamber containing BSA (1.3 nmol/L), Slit3 (0.8 nmol/L), or VEGF (1.5 nmol/L). Slit3-induced HUVEC migration was quantified. The experiments were carried out at least 3 times in triplicate. The data are presented as mean ± SD. ** indicates $P < .001$ when a comparison was made with the wells treated with Slit3 and Ni-Ab by Student *t* test. (B). Soluble extracellular domain of Robo4 (sR4) but not the soluble extracellular domain of Robo1 (sR1) inhibited Slit3-induced HUVEC migration. Slit3- and VEGF-induced HUVEC migration was similarly carried out as described in panel A with supplement of heat-inactivated sR1, heat-inactivated sR4, active sR1, or active sR4 (each at 1 μg) in the lower chamber. Only the active sR4 showed an inhibitory effect on the Slit3-induced HUVEC migration. Furthermore, neither Robo1 nor Robo4 affected the VEGF-directed EC migration. (C). CM collected from HUVEC and VSMC culture induced Robo4-dependent HUVEC migration. The CM was collected from serum-free culture of HUVECs (EC-CM) and VSMCs (VSMC-CM), respectively, and tested for their promigratory activity as described in panel A with or without the addition (1 μg) of Ni-Ab or R4-Ab. The R4-Ab but not the Ni-Ab partially inhibited the CM-induced HUVEC migration, suggesting that endogenous Slit3 interacts with Robo4 to induce EC migration to promote angiogenesis. (D) Slit3 activates Rho GTPases. HUVECs before and after Slit3 stimulation were lysed, and the GST pull-down assays were carried out to quantitate the GTP binding form of endogenous Rho GTPases (the active form, a-). The total Rho GTPases (t-) were detected with corresponding antibody by Western blot analysis. The bands were quantified by density measurement. All the experiments were performed 3 times independently. (E). Anti-Robo4 antibody blocked Slit3-induced activation of Rho GTPases. Ni-Ab (1 μg) or R4-Ab (1 μg) was supplemented in culture medium before HUVECs received Slit3 (0.8 nmol/L) stimulation. After 15 minutes of the Slit3 treatment, the HUVECs were lysed for Rho GTPase analyses. (F) Slit3 triggers actin cytoskeleton reorganization in ECs and formation of stress fiber and lamelipodia. Subconfluent HUVECs were serum-starved overnight, treated with Slit3 (0.8 nmol/L) or BSA (1.3 nmol/L) for 30 minutes, and then stained with TRITC-phalloidin. Fluorescence images were captured at ×20 magnification. Arrowheads indicate actin stress fibers (white) and lamellipodia (green). Scale bar, 20 μm.

anti-Robo4 antibody, but not the nonimmune antibody, blocked Slit3-induced Rac1 and RhoA activation, showing that Slit3 interacts with Robo4 to activate the Rho GTPases in ECs (Figure 5E).

The RhoA pathway is necessary for EC contraction, stress fiber assembly, and inhibition of spreading, whereas Rac1 is required for the formation of actin-rich lamellipodia at the leading edges of polarized cells.[42] The activation of Rac1 and RhoA pathways by Slit3 was further supported by the examination of EC morphology upon Slit3 stimulation. As shown in Figure 5F, BSA-treated HUVECs spread widely with few cells forming lamellipodia. In contrast, Slit3-treated ECs showed typical migrating cell morphology, including cell contraction and formation of multiple lamellipodia. Consistent with these observations, TRITC–phalloidin staining showed that in BSA-treated ECs, no stress fibers trespassed the cytoplasm and few lamellipodia and filopodia were formed at the cellular pole, showing only basal and low levels of RhoA and Rac1 activation, whereas the Slit3-treated ECs formed thick longitudinal stress fibers across the cell body and actin-rich lamellipodia at the leading edges, implying a dramatically increased activation of RhoA and Rac1 signaling. Together, these data demonstrate that Slit3 interacts with Robo4 to activate Rho GTPases to modulate EC motility.

Slit3 promotes angiogenesis in vitro and ex vivo

ECs are capable of forming capillary-like structures on matrigel, a multistep vascular morphogenesis process involving cell adhesion, migration, differentiation, and growth.[25,27,43] To assess whether Slit3 can promote vascular morphogenesis in vitro, HUVECs grown on matrigel-coated wells were treated with BSA (1.3 nmol/L), Slit3 (0.8 nmol/L), VEGF (1.5 nmol/L), or FGF-2 (1.8 nmol/L). After 6 hours of incubation, ECs cultured in Slit3-, VEGF-, and FGF-2–supplemented wells congregated and formed significantly more EC tubes than those cultured with BSA, demonstrating that Slit3 accelerates vascular morphogenesis (Figure 6A). Quantification of TTL revealed that the Slit3, FGF-2, and VEGF treatment induced 3.0-, 4.0-, and 3.5-fold more TTL than the BSA control, respectively (Figure 6B). To test whether Slit3 interacts with Robo4 to modulate the vascular morphogenesis, the tube formation assay was repeated with functional blocking antibody. As shown in Figure 6C-D, anti-Robo4 antibody, but not the nonimmune or the

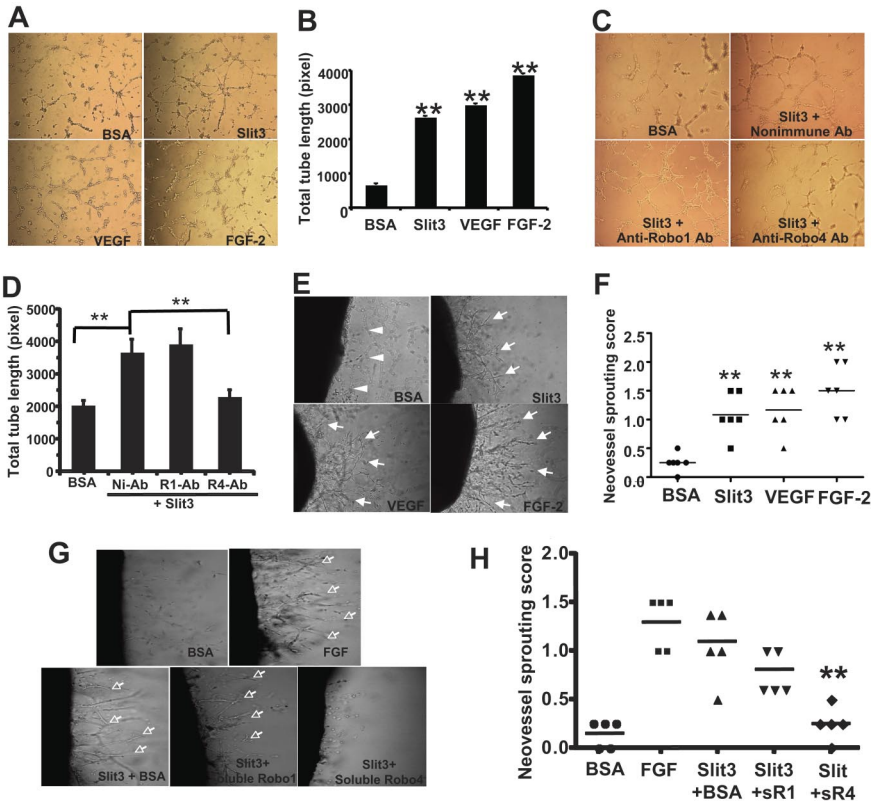

Figure 6. Slit3 induces angiogenesis in vitro and ex vivo. (A) Slit3 induced EC tube formation. HUVECs cultured on growth factor-reduced-matrigel were treated with BSA (1.3 nmol/L), Slit3 (0.80 nmol/L), VEGF (1.5 nmol/L), or FGF-2 (1.8 nmol/L). The images were acquired 6 hours after the treatments. (B). The total tube lengths of panel A were quantified. The data are summarized from experiments performed 3 times in triplicate and are presented as mean ± SD. $*P < .05$ compared with BSA control by Student *t* test. (C-D) The Anti-Robo4 Ab but not anti-Robo1 Ab inhibited Slit3-induced EC tube formation. Slit3-induced HUVEC tube formation was determined as described in panel A in the presence of 2 μg of nonimmune (Ni-Ab), anti-Robo1 (R1-Ab), or anti-Robo4 (R4-Ab) antibody (Ab). (E) Rat aortic ring assay. Rat aortic rings implanted in Matrigel supplemented with BSA (1.3 nmol/L), Slit3 (0.80 nmol/L), VEGF (1.5 nmol/L), or FGF-2 (1.8 nmol/L). The images were acquired 7 days after the treatments. Arrow indicates sprouting neomicrovessels. Arrowhead indicates migrating fibroblast cells. (F) Quantification of the sprouting neovessel followed the criteria described in "Methods." The data are shown as an average score of each treatment ± SD, n = 6 for each test group. $**P < .001$ compared with BSA control by Wilcoxon signed-rank test. (G-H) The soluble extracellular domain of Robo4 but not of Robo1 inhibited Slit3-induced neovascularization in the rat aortic ring assays. Slit3-induced neovascularization was repeated with the rat aortic ring assay in the presence of BSA, soluble Robo1 (sR1), or soluble Robo4 (sR4). BSA and FGF-2 alone served as negative and positive control, respectively. $**P < .001$ compared with Slit3 + BSA group by Wilcoxon signed-rank test. n = 5 per test group.

anti-Robo1 antibody, disrupted Slit3-induced HUVEC tube formation, showing that Slit3 interacts with Robo4 to modulate vascular morphogenesis in vitro.

To determine whether Slit3 initiates the formation of sprouting microvessels from preexisting vessels, a central process of angiogenesis, rat aortic ring assay, was carried out by supplementing the test factors in culture medium for 7 days. As shown in Figure 6E, the negative control BSA-treated aortic rings only had a few observable blood vessels migrating from the adventitia, which were very short with no branching in general. In sharp contrast, Slit3 and VEGF and FGF-2, which served as positive controls, all stimulated robust microvessel sprouting. The induced sprouting neovessels were long, with 2 to 3 degrees of branches. Semiquantification of the sprouting vessels revealed that Slit3 had a proangiogenic activity comparable with VEGF, although weaker than FGF-2 (Figure 6F). We further tested whether Slit3 interacts with Robo4 to initiate the ex vivo neovascularization by adding the anti-Robo4 functional blocking antibody or soluble Robo into the assay. As shown in Figure 6G-H, the addition of anti-Robo4 antibody and soluble Robo4 but not the nonimmune antibody or heat-inactivated soluble Robo4 inhibited Slit3-induced microvessel sprouting, demonstrating that Slit3 interacts with Robo4 to induce microvessel sprouting in the assay. Taken together, these observations demonstrate that Slit3 interacts with Robo4 to modulate angiogenesis and is a potent proangiogenic factor in vitro and ex vivo.

Slit3 stimulates angiogenesis in vivo

To examine whether Slit3 can induce angiogenesis in vivo, CAM and mouse corneal micropocket angiogenesis assays were performed. In the CAM assay, gelfoam soaked with BSA (6.5 nmol/L), Slit3 (4 nmol/L), or FGF-2 (18 nmol/L) was placed on the chorioallantoic membrane of fertilized eggs, and the number of blood vessels sprouting into the sponges was counted after 3 days. As shown in Figure 7A-D, Slit3 and FGF-2 each induced significantly more radial blood vessels that migrated to the sponge than BSA. In the mouse corneal micropocket angiogenesis model, slow-releasing hydron pellets supplemented with Slit3 (1.4 nmol/L) or FGF-2 (6.4 nmol/L) were implanted into one mouse cornea, with the second cornea of the same mouse was used as negative control in which only the blank hydron pellet was implanted. As shown in Figure 7E-H, 5 days after implantation Slit3 and FGF-2 induced limbic vessel looping, dilation, and sprouting. Immunohistologic staining further showed that platelet-EC adhesion molecule-1–positive ECs and platelet-derived growth factor β-receptor (PDGFR)-positive VSMCs/pericytes were recruited in the Slit3-induced neovasculature (Figure 7I-N). In contrast, the control pellets did not induce any corneal angiogenesis. In together, the 2 in vivo angiogenesis models consistently demonstrated that Slit3 is a potent and bona-fide proangiogenic factor.

Deficiency of Slit3 disrupts angiogenesis in developing mouse diaphragm

To test whether Slit3 modulates angiogenesis during development, we further examined Slit3 knockout (*Slit3*$^{-/-}$) mice. The *Slit3*$^{-/-}$ mice exhibit a congenital diaphragmatic hernia (CDH) phenotype, and *Slit3* and *Robo1/4* are expressed in wild-type developing diaphragm (Figure 1A).[24,25] We examined the vasculature of developing diaphragms by whole-mount staining with an anti-mouse PECAM-1 antibody on embryonic day 15.5, a stage when the diaphragm is just formed and before the occurrence of CDH in the *Slit3*$^{-/-}$ mice. As shown in Figure 7O-T, the phenotypically normal *Slit3* heterozygous (*Slit3*$^{+/-}$) diaphragms had an uniform vessel architecture with a regular branching pattern and density, whereas the *Slit3*$^{-/-}$ diaphragms showed tortuous vascular patterns with dramatically reduced density and branches. Quantification revealed that, compared with *Slit3*$^{+/-}$ control, the total vascular

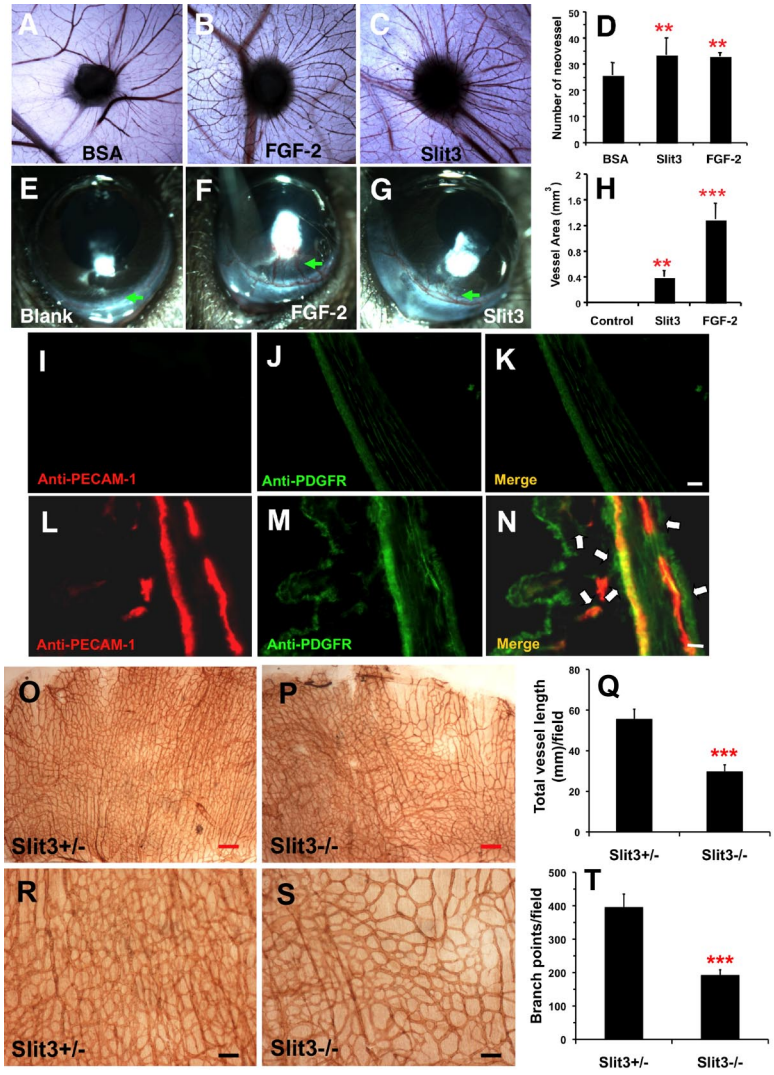

Figure 7. Slit3 promotes angiogenesis in vivo and *Slit3*$^{-/-}$ mice display disrupted angiogenesis in developing diaphragm. (A-D) CAM assay. Gelfoam sponges soaked with Slit3 (4.0 nmol/L), FGF-2 (18 nmol/L), or BSA (6.5 nmol/L) were applied to chorioallantoic membrane. After 72 hours, the membranes around sponges were fixed and dissected out, and the number of vessels sprouting into sponges were counted and represented as mean ± SD (n = 8 for each group). The asterisk indicates a statistically significant increase compared with BSA treatment (**$P < .01$ by Student *t* test). (E-N) Mouse corneal micropocket assay. Hydron pellets containing Slit3 (1.3 nmol/L) or FGF-2 (4.8 nmol/L) were implanted into micropockets of the C57BL/6 mouse cornea. The pellets with only balanced buffers were used as a negative control. On day 5, the corneal neovascularization response to test factors was photographed and quantified. To reduce experimental variation, every mouse was implanted into both eyes with either test-factor or control. n = 8 for each group. Asterisks indicate statistically significant difference in the vessel area of the Slit3-inplanted cornea compared with the control group by Student *t* test (H, **$P < .01$; ***$P < .001$). The mouse corneas were further examined for ECs and pericytes/VSMCs by immunostaining with anti-PECAM-1 (red) and anti-PDGFR (green) antibodies, respectively. The control corneas (I-K) did not show any PECAM-1 position cells, showing that neovascularization was not induced, whereas the Slit3-implanted corneas (L-N) exhibited PECAM-1–positive cells and were covered by PDGFR-positive pericytes/VSMCs (indicated by the arrows), confirming that Slit3 potently induced angiogenesis in cornea. Scale bare = 50 μm. (O-T). Whole-mount staining of embryonic day 15.5 diaphragms of *Slit3*$^{+/-}$ and *Slit3*$^{-/-}$ mice with anti-mouse PECAM-1 antibody. Quantification of the vascular parameter showed that, compared with the phenotypically normal littermate control Slit3$^{+/-}$ diaphragm, the *Slit3*$^{-/-}$ diaphragm showed reduced vascular density and branch points. n = 4-6 for each group. Asterisks indicate statistically significant difference compared with *Slit3*$^{+/-}$ control by Student *t* test (***$P < .001$). Red scale bar = 250 μm; black scale bar = 100 μm.

length and branch points in the *Slit3*$^{-/-}$diaphragms were reduced 46.5% and 51.3%, respectively (Figure 7Q and T), showing genetically that Slit3 functions as a proangiogenic factor to modulate developing angiogenesis.

Discussion

Both blood vessel and nerves are vital channels to and from tissues.[14,15] Recent genetic studies have revealed that vascularization and innervation share similar mechanisms in differentiation, growth, and navigation toward their targets.[17-22] Here we provide new supporting evidence that the repulsive axon guidance molecule Slit3 is a novel and bona-fide proangiogenic factor.

Slit3 was reported to express in the endothelium of mouse lung.[8,23] We extended this finding and observed that *Slit3* is expressed and secreted by both ECs and VSMCs, the 2 major cell types of vasculature. We also observed that Robo1 and Robo4 are universally expressed by ECs in various organs (Figure 1). These findings suggest that Slit3 secreted from VSMCs and ECs may function through both paracrine and autocrine mechanisms to regulate EC functions in angiogenesis. This notion was supported by our finding showing that Slit3 secreted from ECs and VSMCs promoted EC migration (Figure 5C). Interestingly, Slit3 expression in vasculature was observed in lung, brain, diaphragm, and kidney but not in liver and heart, suggesting that the regulatory role of Slit3 in physiologic angiogenesis may occur only in specific organs. *Slit3*$^{-/-}$ mice have normal neuronal development but exhibit malformation of diaphragm and kidney, suggesting that the Slit3 deficiency may retard angiogenesis in diaphragm and kidney during embryonic development, which, in turn, may lead to the malformation of diaphragm and kidney in the *Slit3*$^{-/-}$ mice.[7,9,22] We observed that angiogenesis in the developing diaphragm in *Slit3*$^{-/-}$mice is disrupted (Figure 7O-T), demonstrating directly that Slit3 is proangiogenic in vivo and also highlighting that the localized angiogenesis defect may represent the major cell mechanism underlying the CDH phenotype of the *Slit3*$^{-/-}$ mice.

We unexpectedly found that Slit3, Robo1, and Robo4 are expressed in VSMCs (Figure 1; supplemental Figure 2E-H). This observation agrees with a recent report examining Slit3 expression in human aorta VSMCs[24] and suggests that Slit3 may function similarly through the autocrine and paracrine mechanisms to regulate VSMC function. In angiogenesis, ECs recruit VSMCs/pericytes to form mature vascular structures. Several molecules are known to express in vasculature and be involved in endothelial–pericyte/VSMC interactions, such as transforming growth factor-β, angiopoietin-1, and platelet-derived growth factor.[11,12] The expression of Slit3, Robo1, and Robo4 by both ECs and VSMCs implies

that the Slit3–Robo interaction may be a novel pathway to mediate the cross talk between ECs and VSMCs during vascular maturation in angiogenesis. This finding is supported by our observation that Slit3 recruits both ECs and VSMCs/pericytes to form neovasculature (Figure 7L-N); however, further studies are required to vigorously test this hypothesis.

Cell proliferation is an essential process for formation of neovessels.[11,36] Some axon guidance molecules, such as netrin-1, function as both guidance cues and mitogens for angiogenesis.[29,44,45] Although Slit2 does not affect EC proliferation,[21,22] our results revealed that Slit3 is a potent EC mitogen (Figure 2). This observation is consistent with previous studies in which the authors showed that *Slit3*$^{-/-}$ mesenchymal cells in the central tendon region of mice have reduced proliferation rates[9] and that soluble Robo4 inhibits EC proliferation.[20] Activation of mitogen-activated protein kinases Erk1/Erk2, P38, and AKT pathways are known to mediate the mitogenic effect of growth factors such as VEGF and FGF-2.[25,27,36] We found that Slit3 actually down-regulates Erk1 activation (data not shown), which was consistent with a recent report[46] in which the authors showed Robo4 activation by overexpression attenuates Erk signaling, indicating that Slit3 elicits intracellular signaling pathway(s) other than Erk to induce EC proliferation.

In angiogenesis, ECs sense environmental cues and subsequently convert to migration signaling to follow specific navigational paths.[11,12,14,36] The guidance function of Slits in EC migration has merged but is somewhat controversial. Park et al[22] showed that Slit2 interacts with Robo4 to inhibit EC migration and the inhibitory effect was abolished by Slit2 depletion from the CM, whereas Wang et al[21] observed that Slit2 interacts with Robo1 to attract EC migration, revealing that Slit2 possesses a promigratory property. Interestingly, in our studies we found that Robo4 signaling induced EC migration upon Slit3 stimulation, thus showing a function opposite to Slit2-Robo4 interaction, which suggests that the role of Robo4 in angiogenesis may depend on which Slit ligand it binds. Collectively, these observations suggest that the temporal and spatial expression profiles of Slits and Robos may determine the net role of Slit-Robo interaction in angiogenesis.[7,21,22,34,39]

The authors of early studies[22,34] observed that Robo4 is selectively expressed in developing vasculature during mouse development and at the sites of active angiogenesis, including tumor vessels, suggesting that Robo4 may actively regulate angiogenesis. This finding was confirmed by showing that *Robo4* knockdown zebrafish displayed disrupted intersomitic vessel sprouting[35] and by the evidence that soluble Robo4 blocks angiogenesis in vitro and in vivo[20] and Robo4 signaling is attractive in EC migration.[41] However, ablation of Robo4 in mice did not result in an obvious developmental angiogenesis defect; instead, it revealed a function in stabilizing pathologic angiogenesis,[39] showing that the role of Robo4 varies in different model systems and in different angiogenic processes. In our studies, we found that Slit3 functions as a natural ligand for Robo4 and interacts with Robo4 to promote EC proliferation, migration, tube formation, and microvessel sprouting (Figures 2-7), demonstrating a proangiogenic function for Robo4 in mammals.

Taken together, our in vitro and in vivo findings demonstrate that the repulsive axon guidance molecule Slit3 is a novel and bona-fide proangiogenic factor, providing novel supportive evidence that axon guidance molecules critically regulate angiogenesis. Furthermore, our study also revealed that Slit3 is the functional ligand of Robo4 and that Slit3 interacts with Robo4 to induce angiogenesis. Although our studies have observed the potent role of Slit3 in angiogenesis, further investigations are clearly needed to define whether and how this interaction affects developmental, therapeutic, and pathologic angiogenesis and to explore the potential for treating angiogenesis-related human diseases by manipulating the Slit3–Robo4 interactions.

Acknowledgments

We thank Dr David Ornitz (Washington University School of Medicine) for providing us the *Slit3*$^{-/-}$ mice. We also thank Drs Dean Li (University of Utah) and Jane Wu (Northwestern University Feinberg School of Medicine) for suggestive discussion, and Ms Karen Howard for her English revision of the manuscript.

This work was supported by R01HL093339 from the National Heart, Lung, and Blood Institute (to L.W.) and by R21HD052920 from National Institute of Child Health and Human Development (to J.D.E. and L.W.).

Authorship

Contributions: B.Z., J.D.E., and L.W. designed research; B.Z. and U.M.D. performed research; B.Z. analyzed data; J.G. and R.B. provided vital new reagents and experimental discussions; and B.Z. and L.W. wrote the paper.

Conflict-of-interest disclosure: The authors declare no competing financial interests.

Correspondence: Lianchun Wang, MD, Complex Carbohydrate Research Center, University of Georgia. 315 Riverbend Rd, Athens, GA 30602-4712; e-mail: Lwang@ccrc.uga.edu.

References

1. Wang KH, Brose K, Arnott D, et al. Biochemical purification of a mammalian slit protein as a positive regulator of sensory axon elongation and branching. *Cell.* 1999;96(6):771-784.
2. Li HS, Chen JH, Wu W, et al. Vertebrate slit, a secreted ligand for the transmembrane protein roundabout, is a repellent for olfactory bulb axons. *Cell.* 1999;96(6):807-818.
3. Kidd T, Bland KS, Goodman CS. Slit is the midline repellent for the robo receptor in Drosophila. *Cell.* 1999;96(6):785-794.
4. Brose K, Bland KS, Wang KH, et al. Slit proteins bind Robo receptors and have an evolutionarily conserved role in repulsive axon guidance. *Cell.* 1999;96(6):795-806.
5. Kramer SG, Kidd T, Simpson JH, Goodman CS. Switching repulsion to attraction: changing responses to slit during transition in mesoderm migration. *Science.* 2001;292(5517):737-740.
6. Hohenester E, Hussain S, Howitt JA. Interaction of the guidance molecule Slit with cellular receptors. *Biochem Soc Trans.* 2006;34(Pt 3):418-421.
7. Yuan W, Zhou L, Chen JH, Wu JY, Rao Y, Ornitz DM. The mouse SLIT family: secreted ligands for ROBO expressed in patterns that suggest a role in morphogenesis and axon guidance. *Dev Biol.* 1999;212(2):290-306.
8. Liu J, Zhang L, Wang D, et al. Congenital diaphragmatic hernia, kidney agenesis and cardiac defects associated with Slit3-deficiency in mice. *Mech Dev.* 2003;120(9):1059-1070.
9. Yuan W, Rao Y, Babiuk RP, Greer JJ, Wu JY, Ornitz DM. A genetic model for a central (septum transversum) congenital diaphragmatic hernia in mice lacking Slit3. *Proc Natl Acad Sci U S A.* 2003;100(9):5217-5222.
10. Bagri A, Marin O, Plump AS, et al. Slit proteins prevent midline crossing and determine the dorsoventral position of major axonal pathways in the mammalian forebrain. *Neuron.* 2002;33(2):233-248.
11. Carmeliet P. Angiogenesis in life, disease and medicine. *Nature.* 2005;438(7070):932-936.
12. Jain RK. Molecular regulation of vessel maturation. *Nat Med.* 2003;9(6):685-693.
13. Yancopoulos GD, Davis S, Gale NW, Rudge JS, Wiegand SJ, Holash J. Vascular-specific growth

factors and blood vessel formation. *Nature.* 2000; 407(6801):242-248.

14. Carmeliet P, Tessier-Lavigne M. Common mechanisms of nerve and blood vessel wiring. *Nature.* 2005;436(7048):193-200.
15. Autiero M, De Smet F, Claes F, Carmeliet P. Role of neural guidance signals in blood vessel navigation. *Cardiovasc Res.* 2005;65(3):629-638.
16. Tessier-Lavigne M, Goodman CS. The molecular biology of axon guidance. *Science.* 1996; 274(5290):1123-1133.
17. Gitler AD, Lu MM, Epstein JA. PlexinD1 and semaphorin signaling are required in endothelial cells for cardiovascular development. *Dev Cell.* 2004;7(1):107-116.
18. Serini G, Valdembri D, Zanivan S, et al. Class 3 semaphorins control vascular morphogenesis by inhibiting integrin function. *Nature.* 2003; 424(6947):391-397.
19. Torres-Vázquez J, Gitler AD, Fraser SD, et al. Semaphorin-plexin signaling guides patterning of the developing vasculature. *Dev Cell.* 2004;7(1): 117-123.
20. Suchting S, Heal P, Tahtis K, Stewart LM, Bicknell R. Soluble Robo4 receptor inhibits in vivo angiogenesis and endothelial cell migration. *FASEB J.* 2005;19(1):121-123.
21. Wang B, Xiao Y, Ding BB, et al. Induction of tumor angiogenesis by Slit-Robo signaling and inhibition of cancer growth by blocking Robo activity. *Cancer Cell.* 2003;4(1):19-29.
22. Park KW, Morrison CM, Sorensen LK, et al. Robo4 is a vascular-specific receptor that inhibits endothelial migration. *Dev Biol.* 2003;261(1):251-267.
23. Wu JY, Feng L, Park HT, et al. The neuronal repellent Slit inhibits leukocyte chemotaxis induced by chemotactic factors. *Nature.* 2001;410(6831): 948-952.
24. Liu D, Hou J, Hu X, et al. Neuronal chemorepellent Slit2 inhibits vascular smooth muscle cell migration by suppressing small GTPase Rac1 activation. *Circ Res.* 2006;98(4):480-489.
25. Fuster MM, Wang L, Castagnola J, et al. Genetic alteration of endothelial heparan sulfate selectively inhibits tumor angiogenesis. *J Cell Biol.* 2007;177(3):539-549.
26. Wang L, Fuster M, Sriramarao P, Esko JD. Endothelial heparan sulfate deficiency impairs L-selectin- and chemokine-mediated neutrophil trafficking during inflammatory responses. *Nat Immunol.* 2005;6(9):902-910.
27. Tang N, Wang L, Esko J, et al. Loss of HIF-1alpha in endothelial cells disrupts a hypoxia-driven VEGF autocrine loop necessary for tumorigenesis. *Cancer Cell.* 2004;6(5):485-495.
28. Jiang H, Weyrich AS, Zimmerman GA, McIntyre TM. Endothelial cell confluence regulates cyclooxygenase-2 and prostaglandin E2 production that modulate motility. *J Biol Chem.* 2004; 279(53):55905-55913.
29. Park KW, Crouse D, Lee M, et al. The axonal attractant Netrin-1 is an angiogenic factor. *Proc Natl Acad Sci U S A.* 2004;101(46):16210-16215.
30. Wang LJ, Zhao Y, Han B, et al. Targeting Slit-Roundabout signaling inhibits tumor angiogenesis in chemical-induced squamous cell carcinogenesis. *Cancer Sci.* 2008;99(3):510-517.
31. Diglio CA, Grammas P, Giacomelli F, Wiener J. Angiogenesis in rat aorta ring explant cultures. *Lab Invest.* 1989;60(4):523-531.
32. Ribatti D, Nico B, Vacca A, Presta M. The gelatin sponge-chorioallantoic membrane assay. *Nat Protoc.* 2006;1(1):85-91.
33. Rogers MS, Birsner AE, D'Amato RJ. The mouse cornea micropocket angiogenesis assay. *Nat Protoc.* 2007;2(10):2545-2550.
34. Huminiecki L, Gorn M, Suchting S, Poulsom R, Bicknell R. Magic roundabout is a new member of the roundabout receptor family that is endothelial specific and expressed at sites of active angiogenesis. *Genomics.* 2002;79(4):547-552.
35. Bedell VM, Yeo SY, Park KW, et al. roundabout4 is essential for angiogenesis in vivo. *Proc Natl Acad Sci U S A.* 2005;102(18):6373-6378.
36. Coultas L, Chawengsaksophak K, Rossant J. Endothelial cells and VEGF in vascular development. *Nature.* 2005;438(7070):937-945.
37. Tanno T, Fujiwara A, Sakaguchi K, Tanaka K, Takenaka S, Tsuyama S. Slit3 regulates cell motility through Rac/Cdc42 activation in lipopolysaccharide-stimulated macrophages. *FEBS Lett.* 2007;581(5):1022-1026.
38. Deroanne CF, Hajitou A, Calberg-Bacq CM, Nusgens BV, Lapiere CM. Angiogenesis by fibroblast growth factor 4 is mediated through an autocrine up-regulation of vascular endothelial growth factor expression. *Cancer Res.* 1997;57(24): 5590-5597.
39. Jones CA, London NR, Chen H, et al. Robo4 stabilizes the vascular network by inhibiting pathologic angiogenesis and endothelial hyperpermeability. *Nat Med.* 2008;14(4):448-453.
40. Hussain SA, Piper M, Fukuhara N, et al. A molecular mechanism for the heparan sulfate dependence of slit-robo signaling. *J Biol Chem.* 2006; 281(51):39693-39698.
41. Kaur S, Castellone MD, Bedell VM, Konar M, Gutkind JS, Ramchandran R. Robo4 signaling in endothelial cells implies attraction guidance mechanisms. *J Biol Chem.* 2006;281(16):11347-11356.
42. Philippova M, Ivanov D, Allenspach R, Takuwa Y, Erne P, Resink T. RhoA and Rac mediate endothelial cell polarization and detachment induced by T-cadherin. *FASEB J.* 2005;19(6):588-590.
43. Carmeliet P, Jain RK. Angiogenesis in cancer and other diseases. *Nature.* 2000;407(6801):249-257.
44. Lu X, Le Noble F, Yuan L, et al. The netrin receptor UNC5B mediates guidance events controlling morphogenesis of the vascular system. *Nature.* 2004;432(7014):179-186.
45. Wilson BD, Ii M, Park KW, et al. Netrins promote developmental and therapeutic angiogenesis. *Science.* 2006;313(5787):640-644.
46. Seth P, Lin Y, Hanai J, Shivalingappa V, Duyao MP, Sukhatme VP. Magic roundabout, a tumor endothelial marker: expression and signaling. *Biochem Biophys Res Commun.* 2005;332(2): 533-541.